

Received February 15, 2017, accepted March 7, 2017, date of publication March 10, 2017, date of current version April 24, 2017.

Digital Object Identifier 10.1109/ACCESS.2017.2681201

# A Geometry Surveying Model and Instrument of a Scraper Conveyor in Unmanned Longwall Mining Faces

SHANGQING HAO<sup>1</sup>, SHIBO WANG<sup>1</sup>, REZA MALEKIAN<sup>2</sup>, (Senior Member, IEEE),  
BOYUAN ZHANG<sup>1</sup>, WANLI LIU<sup>1</sup>, AND ZHIXIONG LI<sup>1</sup>

<sup>1</sup>School of Mechanical and Electronic Engineering, China University of Mining and Technology, Xuzhou 221116, China

<sup>2</sup>Department of Electrical, Electronic and Computer Engineering, University of Pretoria, Pretoria 0002, South Africa

Corresponding author: S. Wang (wangshb@cumt.edu.cn)

This work was supported in part by the Funds of the National Natural Science Foundation of China under Grant U1510116 and Grant U1610251, in part by the National Key Basic Research Program of China under Grant 2014CB046301, in part by the Major Program of Coal Base of Shanxi under Grant MJ2014-05, in part by the National Natural Science Foundation of Jiangsu under Grant BK20150202, in part by the National Research Foundation of South Africa under Grant RDYR160404161474, in part by the Priority Academic Program Development of Jiangsu Higher Education Institutions.

**ABSTRACT** To maintain the straightness of an unmanned longwall mining face, a track geometry surveying model of the scraper conveyor was constructed based on the position of the shearer. A surveying instrument was developed employing an inertial measurement unit and axial encoder. Surveying tests were conducted using a longwall mining face mock-up, and the 3-D accuracy of the surveying instrument based on the mean radial spherical error and the spherical error probable (SEP) radius was determined to be 20.78 mm and 16.57 mm, respectively. The accuracy of the surveying system satisfied the requirements of a longwall mining face.

**INDEX TERMS** Geometry surveying, inertial measurement, unmanned longwall mining, scraper conveyor.

## I. INTRODUCTION

Longwall mining is a primary coal extraction method for underground mines that is expected to remain prevalent into the foreseeable future. Mechanized longwall mining primarily involves three types of equipment: a shearer, a scraper conveyor, and hydraulic roof supports, as illustrated in Fig. 1. The shearer travels back and forth along a rail associated with the scraper conveyor between intersecting roadways, and typically cuts a 1 m wide slice of coal from the exposed face. The coal is then conveyed to a conveyor belt located at one of the gate roadways. As the shearer moves across the coal seam, large hydraulic push arms attached to the hydraulic roof supports progressively advance the scraper conveyor and associated shearer rail behind the shearer. The roof supports simultaneously prevent the roof from collapsing onto the shearer and immediate work area. When the shearer advances through the seam, the supports follow, allowing the remnant seam to collapse into the void behind the roof supports [1], [2].

For optimum operation, the longwall face should be straight, and should be perpendicular to the gate roadways.

A straight longwall face minimizes the issues associated with mechanical stress on both the scraper conveyor and roof supports [1]. In a manned longwall face, the face profile was usually controlled through manual observation and operation. Generally, a rope installed along the face is selected as a desired straight line. When the face profile is crooked, mining workers individually adjusted the displacements of each hydraulic push arm of hydraulic roof supports to make the scraper conveyor parallel to the rope under non-production condition. In an unmanned longwall face, it is required to measure the face profile and feed this information back to roof support control systems to achieve a desired face alignment. Until now, there is no a robust method of automatically measuring the face profile consistently during production for longwall mining automation systems. The motivation of the study is to develop a surveying device that can measure the face profile without interrupting production.

According to the longwall mining process, the scraper conveyor acts as the rail of the shearer, and it is connected with the roof supports. Therefore, the orientation and straightness of the longwall face are determined by the spatial geometry of

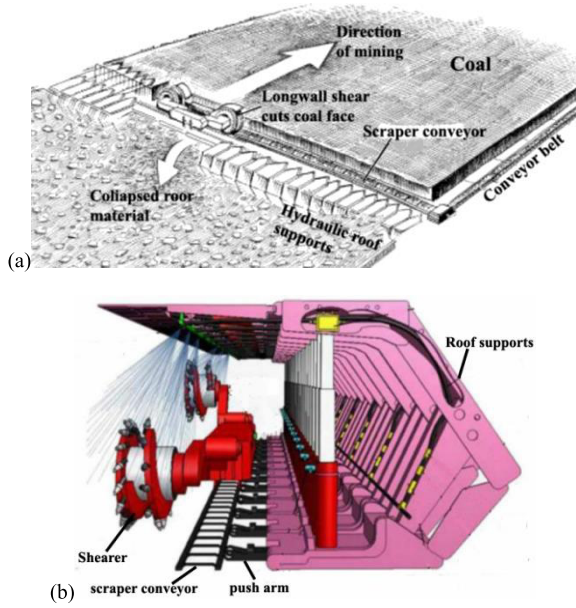


**FIGURE 1.** Typical longwall mining face configuration (a) and equipment employed in a longwall mining face (b) [1].

the scraper conveyor. To realize longwall mining automation, the position of the shearer has been accurately measured with an inertial navigation system (INS) or inertial measurement unit (IMU) [3]–[7]. Because the shearer runs along the scraper conveyor, the spatial geometry of the scraper conveyor can be surveyed through the position of the shearer. As an example, a track geometry surveying method with a trolley equipped with an INS has been used for railway and underground pipeline track surveying [8]–[14].

In the present study, a geometry surveying model of the scraper conveyor is constructed based on an IMU installed on the shearer, and a position measurement instrument is developed according to the model. The model was verified by experiments performed using a longwall mining face mock-up. The longwall face profile can be measured by the model and instrument.

## II. SURVEYING MODEL

Fig. 2 illustrates the spatial relationships between the scraper conveyor and shearer. An IMU and an odometer are mounted on the shearer mainbody and left haulage unit, respectively. The attitude of the shearer mainbody, including the heading angle  $\varphi$ , pitch angle  $\theta$ , and rolling angle  $\gamma$ , is measured by the IMU. The displacement of the shearer is measured by the odometer. According to the principle of inertial navigation, the shearer frame is referred to as the body frame, as shown in Fig. 2(a). The  $X_b$ -axis,  $Y_b$ -axis, and  $Z_b$ -axis are aligned with

$$C_b^n(t) = \begin{bmatrix} \cos \varphi(t) \cos \theta(t) & \cos \varphi(t) \sin \theta(t) \sin \gamma(t) - \sin \varphi(t) \cos \gamma(t) & \cos \varphi(t) \sin \theta(t) \cos \gamma(t) + \sin \varphi(t) \sin \gamma(t) \\ \sin \varphi(t) \cos \theta(t) & \sin \varphi(t) \sin \theta(t) \cos \gamma(t) + \cos \varphi(t) \cos \gamma(t) & \sin \varphi(t) \sin \theta(t) \cos \gamma(t) - \cos \varphi(t) \sin \gamma(t) \\ \sin \theta(t) & -\cos \theta(t) \sin \gamma(t) & -\cos \theta(t) \cos \gamma(t) \end{bmatrix} \quad (3)$$

the pitch, roll, and heading axes, respectively. The local north-east-up (NEU) frame is selected as the navigation frame.

The shearer is carried along the scraper conveyor by four shoes located at points A, B, C, and D in Fig. 2(b) while being hauled by a gear-rack system. The position of the shearer is given by the point denoted as O. The middle points of lines AB and CD, denoted as points M and N, are located on the centerline of the scraper conveyor, as shown in Fig. 2(b). Here, the distance between M and N passing through O is given as  $L_Q$ , and the distance between M and O is given as  $L_M$ . The scraper conveyor is composed of rigid linepan sections, so the centerlines of each linepan reflect the shape of the scraper conveyor. The subpoints of M and N residing on the scraper conveyor, denoted as points  $M_0$  and  $N_0$ , where  $M_0$  is illustrated in Fig. 2(c), represent the spatial geometry of the scraper conveyor. Here, the distance between M and  $M_0$  is given as  $L_H$ . The goal of the surveying model is to obtain the coordinate values of  $M_0$  and  $N_0$  with respect to the coordinate value of O during the shearer running along the scraper conveyor.

### A. POSITION OF THE SHEARER

Dead reckoning for position determination begins from a known initial position and continuously adds relative displacement vectors. This is adopted as the method for determining the position of the shearer. Therefore, the position of the shearer, i.e., the coordinate value of O in the NEU frame, at time  $t_i$ , denoted as  $\mathbf{P}_{nO}(t_i)$ , is determined according to its position at  $t_{i-1}$  by

$$\mathbf{P}_{nO}(t_i) = \mathbf{P}_{nO}(t_{i-1}) + \mathbf{S}_n(t_i) \quad (1)$$

where  $\mathbf{S}_n(t_i)$  is the displacement vector in the NEU frame during a single sampling period, which is calculated as follows.

$$\mathbf{S}_n(t_i) = C_b^n(t_{i-1}) \times \mathbf{S}_b(t_i) = C_b^n(t_{i-1}) \times \begin{bmatrix} \Delta l(t_i) \\ 0 \\ 0 \end{bmatrix} \quad (2)$$

Here,  $\Delta l(t_i)$  is the displacement of the shearer during one sampling period, which is measured by the odometer, and  $C_b^n(t)$  is the transformation matrix from the shearer frame to the NEU frame, which is given by Eq. (3), as shown at the bottom of this page.

### B. POSITION OF THE SCRAPER CONVEYOR

The coordinate of M in the NEU frame, denoted as  $\mathbf{P}_{nM}(t)$ , is determined by

$$\mathbf{P}_{nM}(t_i) = \mathbf{P}_{nO}(t_i) + C_O^M \quad (4)$$

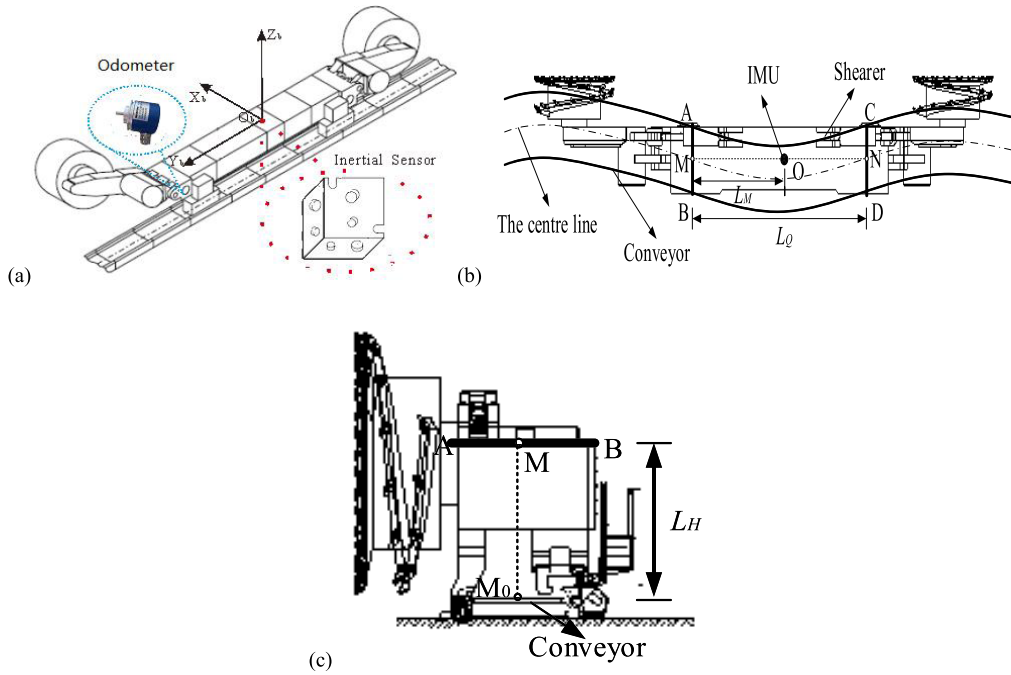


FIGURE 2. The relationship between the scraper conveyor and the shearer fitted with an IMU and odometer.

where  $C_O^M$  is the relationship matrix between M and O in the NEU frame, which is calculated by

$$C_O^M = C_b^n \times R_O^M \quad (5)$$

Here,  $R_O^M$  is the relationship matrix between M and O in the shearer frame, which is defined as  $R_O^M = [-L_M \ 0 \ 0]^T$ .

The position of point  $M_0$  in the NEU frame, denoted as  $P_{nM_0}(t)$ , can be calculated according to  $P_{nM}(t)$  as

$$P_{nM_0}(t) = P_{nM}(t) + C_M^{M_0} \quad (6)$$

where  $C_M^{M_0}$  is the relationship matrix between M and  $M_0$  in the NEU frame, which is calculated by

$$C_M^{M_0} = C_b^n \times R_M^{M_0} \quad (7)$$

Here,  $R_M^{M_0}$  is the relationship matrix between M and  $M_0$  in the shearer frame, which is defined as  $R_M^{M_0} = [0 \ 0 \ -L_H]^T$ .

Combining Eqs. (1–7), the position of  $M_0$  located on the centerline of the scraper conveyor can be determined by Eq. (8), as shown at the bottom of this page, in the NEU frame. Based on the geometrical relationship between  $N_0$  and O, the coordinates of  $N_0$  located on the centerline of the scraper

$$\begin{aligned} P_{nM_0}(t) &= P_{nO}(t_{i-1}) + S_n(t_i) + C_O^M + C_M^{M_0} \\ &= P_{nO}(t_{i-1}) + C_b^n(t_{i-1}) \times S_b(t_i) + C_b^n(t_{i-1}) \times R_O^M + C_b^n(t_{i-1}) \times R_M^{M_0} \\ &= P_{nO}(t_{i-1}) + C_b^n(t_{i-1}) \times (S_b(t_i) + R_O^M + R_M^{M_0}) \\ &= P_{nO}(t_{i-1}) + C_b^n(t_{i-1}) \times \left( \begin{bmatrix} \Delta l(t_i) \\ 0 \\ 0 \end{bmatrix} + \begin{bmatrix} -L_M \\ 0 \\ 0 \end{bmatrix} + \begin{bmatrix} 0 \\ 0 \\ -L_H \end{bmatrix} \right) \\ &= P_{nO}(t_{i-1}) + C_b^n(t_{i-1}) \times \begin{bmatrix} \Delta l(t_i) - L_M \\ 0 \\ -L_H \end{bmatrix} \\ &= P_{nO}(t_{i-1}) + \begin{bmatrix} (\Delta l(t_i) - L_M) \cos \varphi \cos \theta - L_H(\cos \varphi \sin \theta \cos \gamma + \sin \varphi \sin \gamma) \\ (\Delta l(t_i) - L_M) \sin \varphi \cos \theta - L_H(\sin \varphi \sin \theta \cos \gamma - \cos \varphi \sin \gamma) \\ (\Delta l(t_i) - L_M) \sin \theta - L_H(\cos \theta \cos \gamma) \end{bmatrix} \end{aligned} \quad (8)$$

$$P_{nN_0}(t) = P_{nj}(t-1) + \begin{bmatrix} (\Delta l(t_i) + L_Q - L_M) \cos \varphi \cos \theta - L_H(\cos \varphi \sin \theta \cos \gamma + \sin \varphi \sin \gamma) \\ (\Delta l(t_i) + L_Q - L_M) \sin \varphi \cos \theta - L_H(\sin \varphi \sin \theta \cos \gamma - \cos \varphi \sin \gamma) \\ (\Delta l(t_i) + L_Q - L_M) \sin \theta - L_H(\cos \theta \cos \gamma) \end{bmatrix} \quad (9)$$

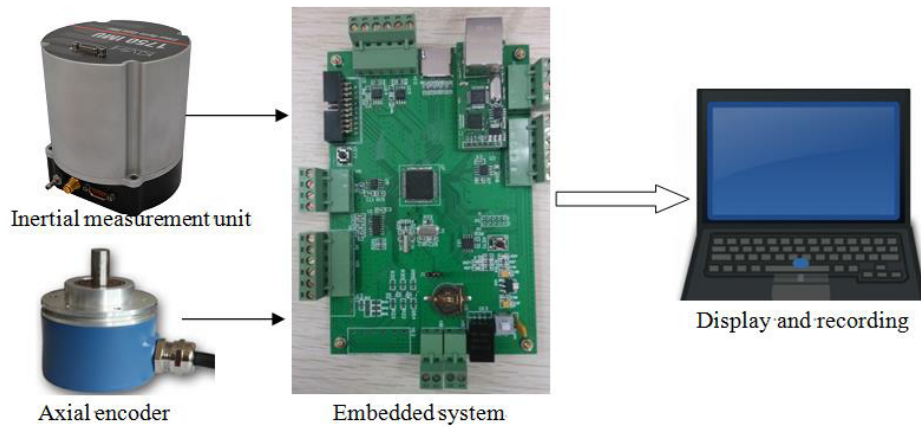


FIGURE 3. Schematic of the conveyor track surveying instrument.

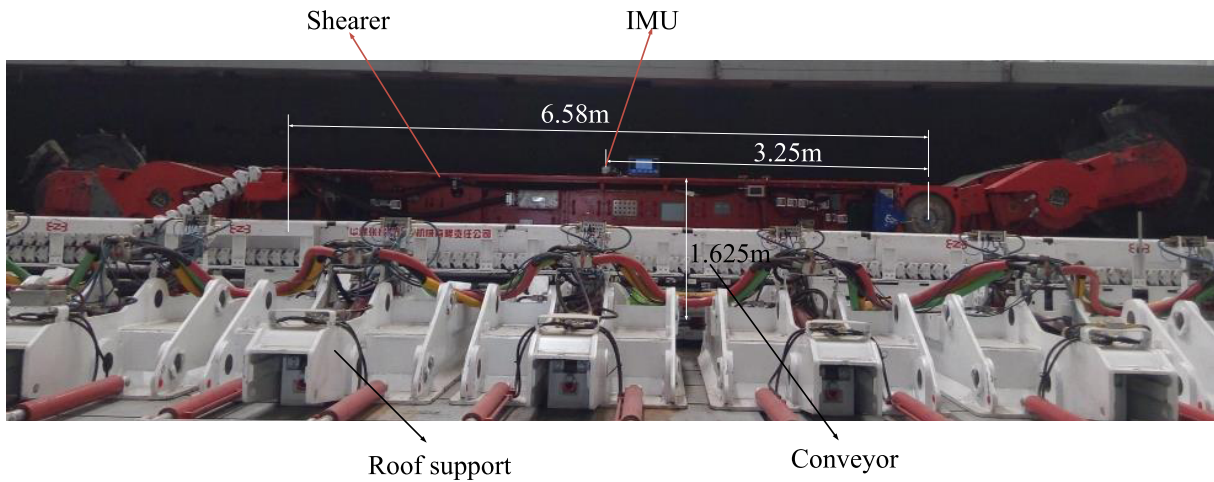


FIGURE 4. The longwall face mock-up constructed with actual mining equipment for experimental testing of the proposed surveying model and corresponding measurement instrument.

conveyor in the NEU frame is determined by Eq. (9), as shown at the bottom of the previous page, which was derived following  $M_0$ . The spatial geometry of the whole scraper conveyor is reconfigured by fusing the position of points  $M_0$  and  $N_0$ . With this measure method, the spatial profile of the scraper conveyor can be surveyed during the shearer continuous productive process. According to the measured profile of the scraper conveyor, the displacements of hydraulic push arms of hydraulic roof supports can be automatically adjusted during advancing the scraper conveyor so that the straightness of the scraper conveyor can be maintained under production condition. This will not only enhance the safety but also increase productivity for coal mine.

### III. EXPERIMENTS

#### A. THE SURVEYING INSTRUMENT HARDWARE

The hardware of the surveying instrument includes an IMU, axial encoder and an embedded system, as shown in Fig.3. The IMU contains a high precision 3-axis accelerometer and

3 high precision gyroscopes, allowing movement in all of the 6 degrees of freedom to be measured. It was installed on the shearer mainbody and used to determine the attitude of the shearer. An incremental axial encoder with the resolution of 4096 pluses per revolution was connected with the haulage unit to measure the displacement. An embedded system was developed for data acquisition and processing according to the surveying model.

Kinematic surveys of a scraper conveyor are characterized by the movement of the shearer. However, the sensors do not sample the data continuously, but are time and value-discrete. Therefore, the sampling frequency, which is the inverse of the time increment  $\Delta t_{sampling}$  between each sampling point, must be related to the speed of the shearer. A conveyor is comprised of numerous linepan sections, which act as the guide rail for the shearer. The geometry of the scraper conveyor was determined by the attitude of each linepan. Each linepan is a rigid body of length  $l = 1000\text{--}2000$  mm. Therefore, the attitude of a single linepan can be determined by two points



FIGURE 5. Installation of the IMU and axial encoder on the shearer.

TABLE 1. Differences between the actual and surveyed tracks shown in Figs. 6(a) and (b).

Direction	Max. (mm)	Min. (mm)	Mean (mm)	Std. Dev. (mm)	MRSE (mm)	SEP (mm)
East (a)	16.4	0.3	7.12	8.81		
North (a)	17.5	1.0	11.52	13.12	16.31	13.25
Up (a)	8.5	0	3.03	4.05		
East (b)	21.9	0.1	9.83	11.80		
North (b)	28.1	0.8	14.06	16.62	20.78	16.57
Up (b)	8.4	0.1	3.06	4.07		

TABLE 2. Differences between the actual and surveyed tracks shown in Fig. 7.

Direction	Max. (mm)	Min. (mm)	Mean (mm)	Std. Dev. (mm)	MRSE (mm)	SEP (mm)
East	31.8	0.2	13.97	16.27		
North	22.3	0.5	8.91	11.05	20.09	16.02
Up	9.2	0.1	3.18	4.08		

along its length. The speed  $v$  of the shearer is usually less than 10 m/min. To obtain two sensor data samples for each linepan during shearer operation, the sampling frequency is

$$f_{sampling} = \frac{1}{\Delta t_{sampling}} \geq \frac{2}{l/v} \quad (10)$$

Under extreme conditions where  $l$  is equal to 1000 m and  $v$  is equal to 10 m/min,  $f_{sampling}$  must be greater than 1/3 Hz. As such,  $f_{sampling}$  is set as 2 Hz in the surveying instrument. The median absolute deviation (MAD) filtering technique is used for outlier detection [10].

**B. EXPERIMENTAL TEST**

To verify the surveying model and test the accuracy of the designed surveying instrument, experiments were

performed using a longwall face mock-up, which included a MG500/1130-WD shearer, a SGZ1000/1050 scarper conveyor, and ZY9000/15/28D roof supports, as shown in Fig. 4. The total length of the conveyor was 60 m and each linepan was 1.75 m in length. The distance between the haulage units was 6.58 m. The height of the shearer was 1.625 m. The installation of the IMU and axial encoder was shown in Fig. 5. A local NEU frame with the origin at the tail end of the scraper conveyor was constructed. The actual geometry of the conveyor was manually measured by an electronic total station with reference to the local NEU frame. The surveying instrument installed on the shearer automatically measured the geometry of the conveyor according to the constructed surveying model during the shearer running along the scraper conveyor. The maximum, minimum, and mean values and

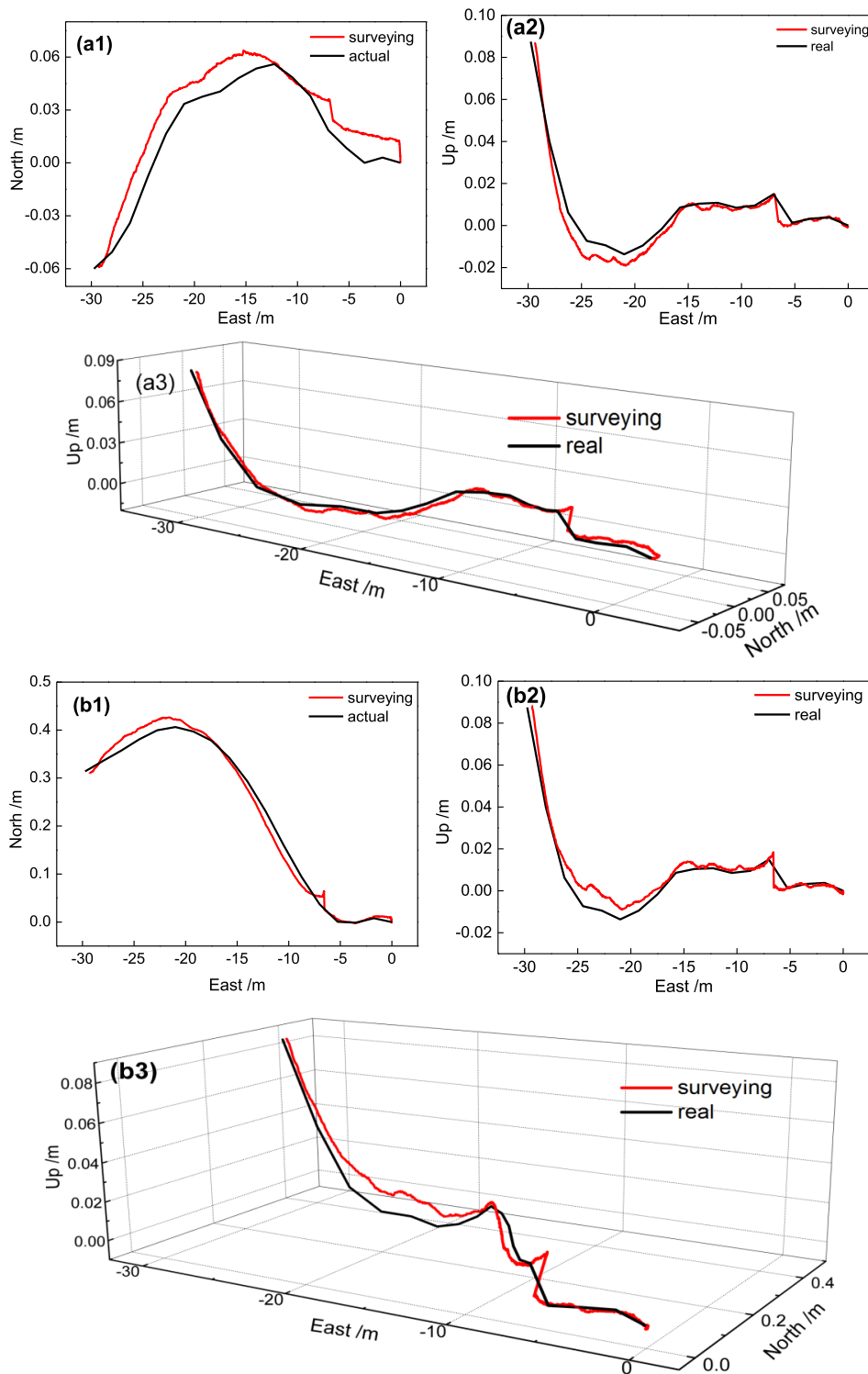


**FIGURE 6.** The actual and surveyed tracks of the scraper conveyor over a 30 m length under linear (a) and curving (b) conditions.

standard errors related to the differences between the actual and surveyed geometry were analyzed to determine the accuracy of the surveying instrument.

The actual and surveyed tracks of the scraper conveyor under different conditions are shown in Figs. 6 and 7.

The close agreement between the surveyed and actual conveyor tracks demonstrates the validity of the proposed model. The maximum, minimum, and mean values and standard deviations related to the differences between the actual and surveying tracks were calculated and listed in

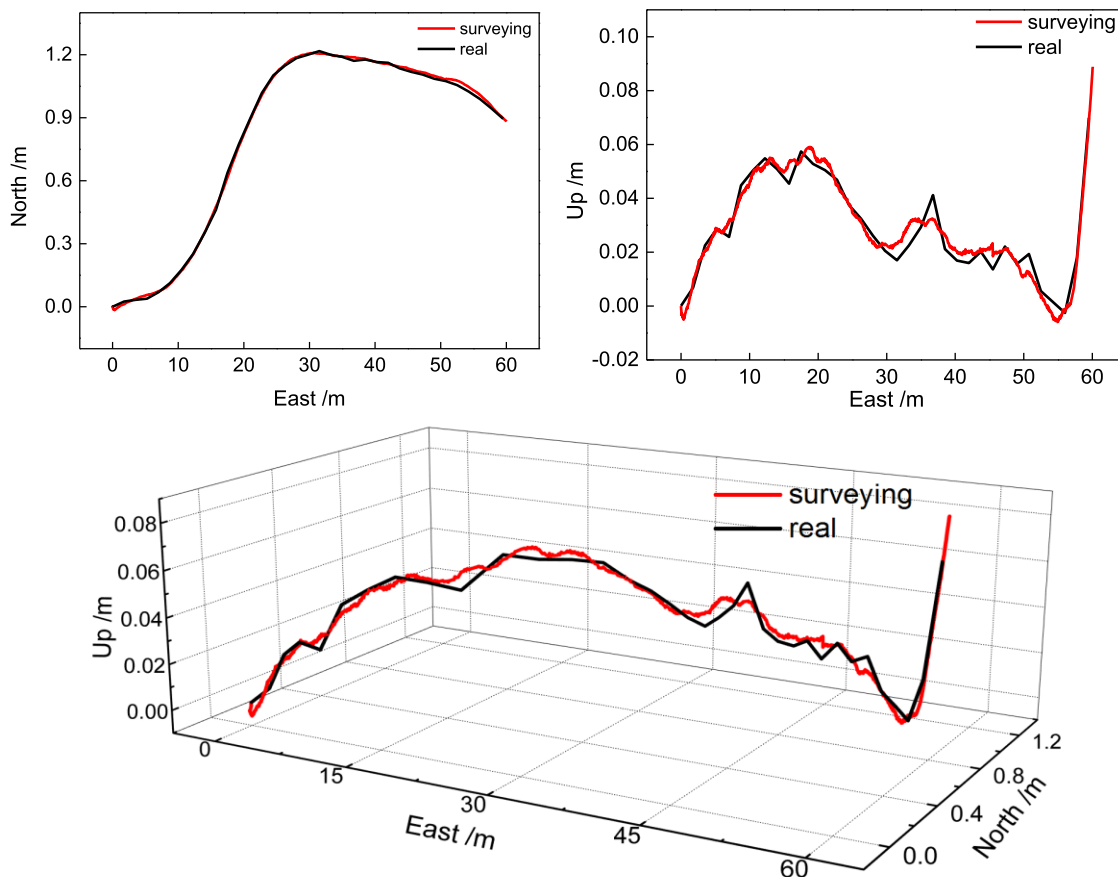


FIGURE 7. The actual and surveyed tracks of the scraper conveyor over a 60 m length under curving conditions.

Table 1 and Table 2. In the NEU coordinate system, the errors in the up-coordinate axis were less than those in the other two coordinate axes. Ideally, the IMU is installed with the sensor axes perfectly aligned with the shearer axes; however, misalignment is inevitable, particularly for the  $X_b$  and  $Y_b$  axes (Fig. 2), which is denoted as heading deviation. The position error of the shearer is greatly affected by heading deviation [4], which correspondingly induced the greater measurement errors observed in the east and north coordinate axes.

To estimate the accuracy of the surveying instrument in three dimensions, a global positioning system (GPS) position accuracy specification was adopted, namely, the spherical error probable (SEP) radius and the mean radial spherical error (MRSE) [15], [16]. The SEP radius is the radius of a sphere centered at the true position [17], containing the position estimate [18], [19] in three dimensions with a probability of 50%. The SEP is calculated as

$$SEP = 0.51(\sigma_N + \sigma_E + \sigma_U) \tag{11}$$

where  $\sigma_N$ ,  $\sigma_E$ , and  $\sigma_U$  are the standard errors in the north, east, and up coordinate axes, respectively. The MRSE is the radius of a sphere centered at the true position, containing the position estimate in three dimensions with a probability

of 61%, and is calculated as

$$MRSE = \sqrt{\sigma_N^2 + \sigma_E^2 + \sigma_U^2} \tag{12}$$

The SEP radius and MRSE values for the data given in Figs. 6 and 7 are listed in Table 1 and Table 2. For a linear scraper conveyor with 30m length (Fig.6 a), the MRSE and SEP are 16.31mm and 13.25mm, respectively. For a curving scraper conveyor with 30m length (Fig.6 b), the MRSE and SEP increase to 20.78mm and 16.57 mm, respectively. The surveying error under curving condition is higher than that under linear condition. The function surveying device is measuring the profile of a curving scraper conveyor accurately so that the support control system adjusts the scraper conveyor to a desired line. So the surveying test with 60m length scraper conveyor was conducted under curving condition. The MRSE and SEP are 20.09 mm and 16.02 mm for a curving scraper conveyor with 60m length (Fig.7). They are similar to that of 30m-length curving scraper conveyor. According to the experiment result, the maximum values of the MRSE and SEP obtained from all the experiments are 20.78 mm and 16.57 mm, respectively. According to the quality management rules of a longwall mining face [20]–[23], a longwall mining face cannot deviate from straightness by an amount greater than 100 mm [24], [25]. It means that the deviation

between the surveyed and actual conveyor tracks [26], [27] is less than 100mm. The accuracy of the surveying system therefore satisfies the requirements of a longwall mining face.

#### IV. CONCLUSIONS

In this paper, a track geometry surveying model of a scraper conveyor was constructed based on the position of the shearer, which was determined by the dead reckoning method. A surveying instrument was developed that included an IMU and an axial encoder. The sampling frequency was determined according to the length of each conveyor linepan and the shearer speed. Surveying tests were conducted using a longwall mining face mock-up, and the accuracy of the surveying instrument in three dimensions based on the MRSE and the SEP radius was evaluated as 20.78 mm and 16.57 mm, respectively. The accuracy of the surveying system satisfied the requirements of a longwall mining face. With the surveying model and the measurement instrument, the spatial profile of the scraper conveyor can be automatically surveyed during the shearer continuous productive process. According to the measured profile, the straightness of the scraper conveyor can be maintained by hydraulic roof supports under production condition. This will not only enhance the safety but also increase productivity for coal mine.

#### REFERENCES

- [1] P. B. Reid, M. T. Dunn, D. C. Reid, and J. C. Ralston, "Real-world automation: New capabilities for underground longwall mining," in *Proc. Australasian Conf.*, Dec. 2010, pp. 1–8.
- [2] B. H. G. Brady and E. T. Brown, "Longwall and caving mining methods," in *Rock Mechanics for Underground 294 Mining*. Champ, The Netherlands: Springer, 2007, pp. 430–483.
- [3] D. C. Reid, D. W. Hainsworth, J. C. Ralston, R. J. McPhee, and C. O. Hargrave, "Inertial navigation: Enabling technology for longwall mining automation," *Comput. Appl. Minerals Ind.*, Oct. 2014, pp.1–5.
- [4] S. Q. Hao, A. Li, S. B. Wang, Z. L. Ge, Z. Z. Zhang, and S. R. Ge, "Effects of shearer inertial navigation installation noncoincidence on shearer positioning error," *J. China Coal. Soc.*, vol. 40, no. 8, pp. 1963–1968, 2015.
- [5] J. Ralston, D. Reid, C. Hargrave, and D. Hainsworth, "Sensing for advancing mining automation capability: A review of underground automation technology development," *J. China Minerals Technol.*, vol. 24, no. 3, pp. 305–310, 2014.
- [6] S. R. Ge et al., "Study on positioning and orientation of a shearer based on geographic information system," *J. China Coal. Soc.*, vol. 40, no. 11, pp. 2503–2508, 2015.
- [7] Z. Z. Zhang, S. B. Wang, B. Y. Zhang, and A. Li, "The shape detection of scraper conveyor based on the shearer trajectory," *J. China Coal. Soc.*, vol. 40, no. 11, pp. 2514–2521, 2015.
- [8] C. Jekeli, *Inertial Navigation Systems With Geodetic 318 Applications*. Berlin, Germany: Walter de Gruyter, 2001.
- [9] R. Glaus, "Kinematic track surveying by means of a multi-sensor platform," Ph.D. dissertation, Inst. Geodesy Photogramm., ETH, Swiss Federal Inst. Technol. Zurich, Zürich, Switzerland, 2006.
- [10] G. J. Yeo, P. F. Weston, and C. Roberts, "The utility of continual monitoring of track geometry from an in-service vehicle," in *Proc. IEEE RCM Conf.*, Birmingham, U.K., Sep. 2014, pp. 1–6.
- [11] J. J. He, "Development of path measuring and plotting with underground utility," *J. Shanghai Elect. Power*, vol. 27, no. 3, pp. 285–288, 2011.
- [12] B. Akpınar, "A new measurement system design for determining the geometrical changes on railways," Ph.D. dissertation, Geomatics Eng., Yildiz Tech. Univ., Istanbul, Turkey, 2009.
- [13] Y. Yang, X. J. Wu, L. J. Yang, and B. Li, "Inspection of three-dimensional geographic coordinate in pipeline," *Opt. Precis. Eng.*, vol. 22, no. 10, pp. 2740–2745, 2014.
- [14] E. H. Shin and N. El-Sheimy, "Navigation Kalman filter design for pipeline piggings," *J. Navigat.*, vol. 58, no. 2, pp. 283–295, 2005.
- [15] N. Singh, "Spherical probable error (SPE) and its estimation," *Proc. Metrika*, vol. 15, no. 1, pp. 149–163, 1970.
- [16] J. Cline, "Two new measures of position error," *IEEE Trans. Aerosp. Electron. Syst.*, vol. 12, no. 2, pp. 291–292, Mar. 1976.
- [17] J. H. Wang, L. T. Huang, S. B. Li, and Z. H. Huang, "Development of intelligent technology and equipment in fully-mechanized coal mining face," *J. China Coal. Soc.*, vol. 39, no. 8, pp. 1418–1423, 2014.
- [18] J. F. Niu, "Research of straightness control system of fully-mechanized coal mining face," *Ind. Mining Automation*, vol. 41, no. 5, pp. 5–8, 2015.
- [19] V. Henriques, "Mine safety system using wireless sensor network," *IEEE Access*, vol. 4, pp. 3511–3521, 2016.
- [20] B. Su, J. Yu, X. Feng, and Z. Liu, "Electrical anisotropic response of water conducted fractured zone in the mining goaf," *IEEE Access*, vol. 4, pp. 6216–6224, 2016.
- [21] Z. Wang, N. Ye, R. Wang, and P. Li, "TMicroscope: Behavior perception based on the slightest RFID tag motion," *Elektron. Elektrotech.*, vol. 22, no. 2, pp. 114–122, 2016.
- [22] X. Li, S. Wang, S. Hao, and Z. Li, "Numerical simulation of rock breakage modes under confining pressures in the rock cutting process: An experimental investigation," *IEEE Access*, vol. 4, pp. 5710–5720, 2016.
- [23] X. Jin, J. Shao, X. Zhang, and W. An, "Modeling of nonlinear system based on deep learning framework," *Nonlinear Dyn.*, vol. 84, no. 3, pp. 1327–1340, 2016.
- [24] R. Malekian, D. C. Bogatinoska, A. Karadimce, J. Trengoska, and W. A. Nyako, "A novel smart ECO model for energy consumption optimization," *Elektron. Elektrotech.*, vol. 21, no. 6, pp. 75–80, 2015.
- [25] J. Shao, L. Wang, W. Zhao, and Y. Zhong, "An improved synchronous control strategy based on fuzzy controller for PMSM," *Elektron. Elektrotech.*, vol. 20, no. 6, pp. 17–23, 2014.
- [26] K. M. Modieginyane and B. B. Letswamotse, "Software defined wireless sensor networks (SDWSNs) application opportunities for efficient network management: A survey," *Comput. Elect. Eng. J.*, to be published.
- [27] Z. Wang, N. Ye, F. Xiao, and R. Wang, "TrackT: Accurate tracking of RFID tags with mm-level accuracy using first-order Taylor series approximation," *AD Hoc Netw.*, vol. 53, pp. 132–144, 2016.



**SHANGQING HAO** received the M.S degree in fluid power engineering from the Lanzhou University of Technology. He is currently a Senior Engineer and the Vice-President with Shanxi TZ Coal Mine Whole-set Equipment Co., Ltd. His research interests include mining machinery and intelligent mining equipment.



**SHIBO WANG** received the Ph.D. degree in mechanical design and theory from the China University of Mining and Technology, Xuzhou, China, in 2007. He is currently a Professor with the China University of Mining and Technology. His research interests include tribology and intelligent mining equipment. He was the Committee Member of the ninth and tenth tribology section of the Chinese Mechanical Engineering Society.



**REZA MALEKIAN** (M'10–SM'17) is currently an Associate Professor with the Department of Electrical, Electronic, and Computer Engineering, University of Pretoria, Pretoria, South Africa. His research interests include the design and development of industrial applications using advanced sensor networks and Internet of Things. From 2013 to 2016, he has been a Management Committee Member of the ICT COST Action IC1304 Autonomous Control for a Reliable Internet of Services. He is also a Chartered Engineer registered in Engineering Council of U.K., and a Professional Member of the British Computer Society.



**WANLI LIU** received the Ph.D. degree from Tianjin University. He is currently an Associate Professor and a Master Tutor with the School of Mechanical and Electrical Engineering, China University of Mining and Technology. His research interests include laser technology and intelligent mining equipment.



**BOYUAN ZHANG** is currently pursuing the master's degree with the School of Mechanical and Electrical Engineering, China University of Mining and Technology. His research interests include mining machinery and intelligent mining equipment.



**ZHIXIONG LI** is currently a Senior Lecture with the China University of Mining and Technology, China. His research interests include mechanical systems and signal processing. He is an Editorial Member of *Advances in Science and Technology Research Journal* and Recent Patents on Mechanical Engineering.

...